

The IceCube Project

C. Spiering for the IceCube Collaboration *

DESY Zeuthen, Platanenallee 6, D15739 Zeuthen, Germany
christian.spiering@desy.de

Abstract

This talk gives a brief description of goals, design, expected performance and status of the IceCube project.

I. PHYSICS GOALS

The main goal of the IceCube project [1] is to extend the region of the Universe explored by neutrinos and thereby to test fundamental laws of physics, to obtain a different view of astronomical objects, and to learn about the origin of the highest-energy cosmic rays.

Science topics include the search for steady and variable sources of high energy neutrinos like Active Galactic Nuclei (AGN), Supernova Remnants (SNR) or microquasars, as well as the search for neutrinos from burst-like sources like Gamma Ray Bursts (GRB). The sensitivity of IceCube to astrophysical sources of high energy muon neutrinos is described in [2] and in Section V.

Similar to the Mediterranean projects discussed at this workshop, IceCube can also tackle a series of questions beside high energy neutrino astronomy. They include the search for neutrinos from the decay of dark matter particles (WIMPs) and the search for magnetic monopoles or other exotic particles like strange quark matter or the Q-balls predicted by SUSY models (see for reviews [3, 4]).

There are, however, two modes of operation which are not – or nearly not – possible for detectors in natural water. Firstly, due to the low light activity of the surrounding medium, the PMT counting rate is below 1 kHz. This enables the detection of feeble rate increases as caused, for instance, by interactions of Supernova burst neutrinos. IceCube can monitor the full Galaxy for MeV neutrinos from Supernova explosions. Secondly, IceCube can be operated in coincidence with a surface air shower array, IceTop. This allows to study questions like the chemical composition of cosmic rays up to 10^{18} eV, to calibrate IceCube, and to use IceTop as a veto for background rejection.

II. DETECTOR CONFIGURATION

The configuration of IceCube is shown in Fig. 1. IceCube is an array of 4800 optical modules (OMs) on 80 strings, regularly spaced by 125 m. It covers an area of approximately 1 km^2 , with the OMs at depths of 1.4 to 2.4 km below surface. Each

string carries 60 OMs, vertically spaced by 17 m. The strings are arranged in a triangular pattern. At each hole, one station of the IceTop air shower array will be positioned. An IceTop station consists of two ice tanks of total area 7 m^2 . Two of these tanks are being installed during the current (2003/04) season.

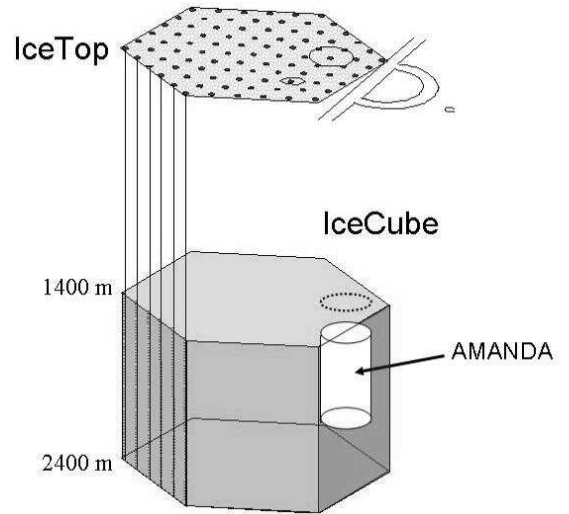


Figure 1: IceCube, IceTop and Amanda

The present Amanda-II detector [5] will be integrated into IceCube. The present runway as well as the old South Pole station, buried not far from Amanda under the snow, prevent an extension of IceCube into the corresponding area and therefore a central location of Amanda within IceCube. Still, IceCube will deliver efficient veto information for low energy cascade-like events or short horizontal tracks recorded in Amanda. Horizontal tracks could be related to neutrinos stemming from WIMP annihilations in the Sun.

Various configurations with the number of OMs ranging from 2400 (half the design number) to 9600 (twice the design number), with equally spaced strings and with nested subarrays of larger density, and also a variety of “exotic” configurations have been studied in detail [6]. The present configuration is tailored for best sensitivity to muon neutrinos in the energy range of TeV-100 TeV. Better sensitivity at low energy may be obtained by improved sensitivity of individual OMs (i.e. by application of wave length shifters [7], see below). Better sensitivity at higher energies as obtained by *additional* strings along sparsely equipped circle(s) around IceCube is discussed in [8].

*a full author list is given at the end of this paper

III. THE DIGITAL OPTICAL MODULE

The IceCube optical module is sketched in Figure 2. It contains a 10-inch diameter PMT HAMAMATSU R-7081. The main argument for this choice was, apart from excellent charge and time resolution, the low noise of a only few hundred Hz (at temperatures of -20 to -40 °C). Low dark noise of the PMTs is not a strong criterion for water detectors since in natural water the ambient noise dominates. In ice, PMTs can be operated without tight local coincidences if only their noise is smaller than a few kHz. A compromise with respect to noise would significantly deteriorate the performance, in particular for detection of low-energy Supernova neutrinos. The PMT is embedded in a transparent gel and shielded against the Earth's magnetic field by a mu-metal grid.

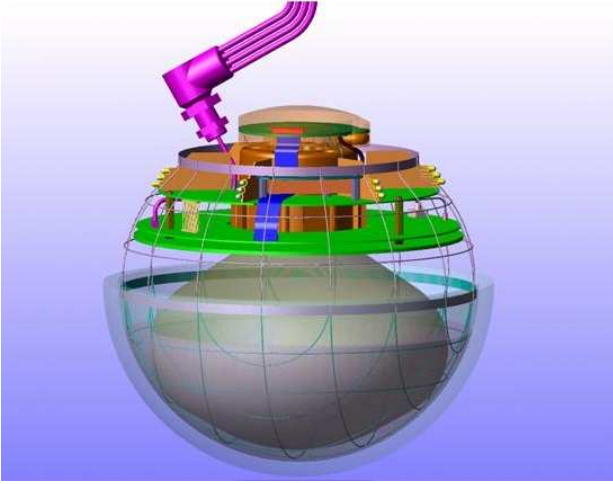


Figure 2: Schematic view of the IceCube DOM

The PMT anode signal (gain $\sim 5 \cdot 10^7$) is digitized within the OM (or Digital Optical Module, DOM) and sent to surface via electrical twisted-pair cables, one twisted pair for two DOMs. The DOM contains several electronic components: the signal processing board, a LED flasher board for calibration purposes, and the PMT base with the high voltage power supply.

The requirements for time resolution and dynamic range are:

- waveform recorded with 250 MHz over the first $0.5 \mu\text{s}$ and 40 MHz over $5 \mu\text{s}$.
- each pulse time stamped with 7 ns r.m.s.
- dynamic range 200 photoelectrons over first 15 ns and 2000 photoelectrons when integrated over $5 \mu\text{s}$.
- dead time $< 1\%$
- noise rate < 500 Hz.

The fine sampling is done with the Analog Transient Waveform Recorder (ATWR), an ASIC with four channels, each capable to capture 128 samples with 200-800 Hz. The 40 MHz sampling is performed by a commercial FADC.

The effects of light scattering on the photon arrival time are dominant compared to effects of PMT jitter and time calibration. It has been shown that reconstruction quality only worsens if the jitter increases beyond 10-15 ns, resulting in a design value of 7 ns for overall timing accuracy. Time calibration over 2-3 km electrical cable with a few-nanosecond accuracy is a challenge. In IceCube it is solved by sending a bipolar signal from the DAQ to the DOM (see Fig. 3, left). The leading edge of this signal is synchronized to the surface clock common to all DOMs. The signal is considerably dispersed over 2 km cable and is subject to baseline variations and noise. Therefore the calibration signal arriving at the DOM is digitized by a FADC. The full waveform information allows for a correction with respect to the mentioned effects. Since the stability of the local oscillator in the DOM is better than 10^{-10} , the calibration process has to be repeated only every 10 seconds.

The time offset is determined by a method known as Reciprocal Active Pulsing (RAP) [9]. In response to the calibration signal, after a well-defined delay δt , the same bipolar signal is sent back to surface and treated there in exactly the same way as the downward calibration signal had been treated in the DOM. This procedure yields an overall delay $T_{\text{roundtrip}}$. With the same signal treatment at surface and in the DOM, one gets $T_{\text{up}} = T_{\text{down}} = 0.5(T_{\text{roundtrip}} - \delta t)$. This information defines the time offset for each DOM and can be determined by multiple round trip measurements with better than 1 ns accuracy. Overall, the instantaneous accuracy of the time calibration is expected to be 5 ns r.m.s.

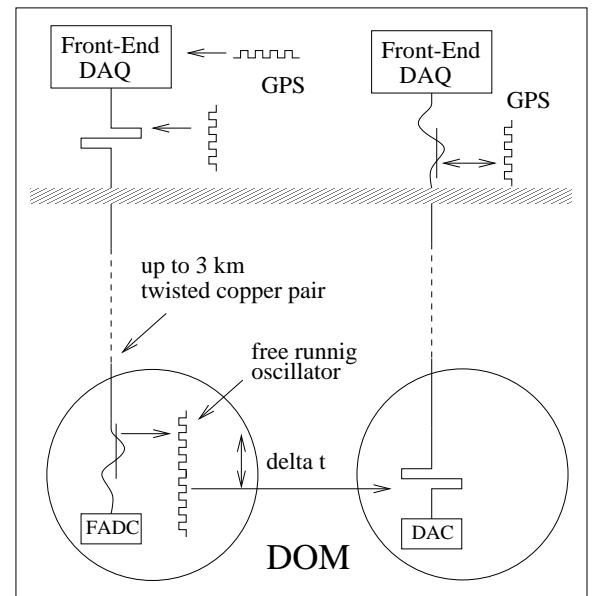


Figure 3: Principle of time calibration and offset determination

IV. DRILLING AND DEPLOYMENT

The drill technology for IceCube is well understood from experience with several years of Amanda deployments. Holes of 60 cm diameter are drilled with 80 °C hot water. For IceCube, a new drilling system (Enhanced Hot Water Drill, EHWD) has been constructed. The power for heaters and pumps of the EHWD will be ~ 5 MW, compared to 2 MW for Amanda. This, and larger diameter and length of the water transporting hoses, will result in only 40 hours needed to drill a 2400 m deep hole (three times faster than with the old Amanda drill). The fuel consumption is reduced by one third.

Mounting, testing and drop of a string with 60 DOMs is expected to take about 20 hours. Since the set-up of the drilling and deployment system at the beginning of the Antarctic summer season will be reduced from 5 to 3 weeks, deployment of 16 strings per season is feasible.

V. PHYSICS PERFORMANCE

In this section, we summarize results on *track* detection at TeV to PeV energies published in [2]. IceCube performance at higher energies is considered in [11].

Figure 4 (top) shows the effective area after $\sim 10^{-6}$ reduction of events from downward muons as a function of the muon zenith angle. Whereas at TeV energies IceCube is blind towards the upper hemisphere, at PeV and beyond the aperture extends above the horizon and allows observation of the Southern sky. Figure 4 (bottom) shows the effective area as function of the muon energy at the detector, averaged over the lower hemisphere. The upper curves refer to events passing trigger criteria (triangles) and fake event reduction (full circles). The other two curves show the effective area after tuning the cuts for best sensitivity to hypothetical steady point source fluxes which follow E^{-2} (stars) and $E^{-2.5}$ (diamonds) power laws, respectively. The threshold is around 1 TeV for E^{-2} spectra. The energy-dependent optimum cut is applied to N_{ch} , the number of fired PMTs.

Fig. 5 shows the pointing resolution for neutrino-induced muon events after background rejection and assuming an E^{-2} spectrum. For not too steep angles the resolution is 0.6 to 0.8 degrees, improving with energy. We expect that evaluation of waveform information will improve these numbers significantly, at least at high energies. Paradoxically, the reason is the strong light scattering which is known to be a clear drawback with respect to the accuracy of first-photon arrival times. Part of this drawback can likely be turned into an advantage since scattering modifies the arrival time distribution as a function of distance between source and receiver. A wider distribution of a many-photoelectron signal recorded by a single PMT indicates a more distant source [12]. This additional information can be used to improve reconstruction, provided the amount of light is high enough to generate multi-photoelectron waveforms in many PMTs. However, a resolution as good as projected for water detectors seems hardly achievable.

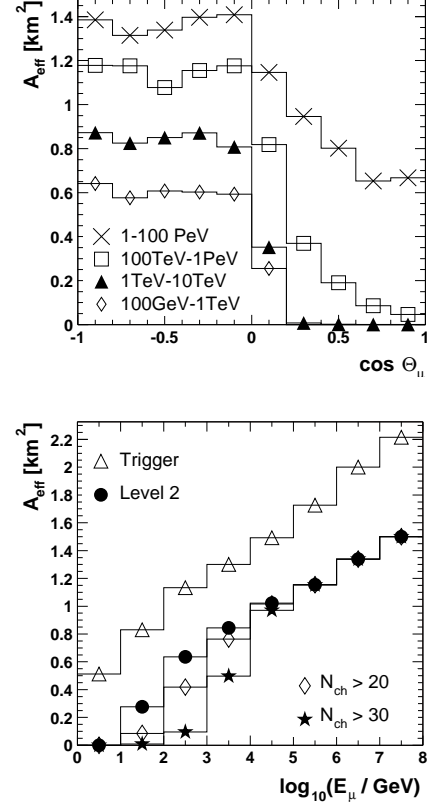


Figure 4: Effective area for muon as a function of zenith angle (top) and as a function of muon energy (bottom). The lower figures refers to muons from the lower hemisphere ($\cos \theta < 0$). See text for further explanations.

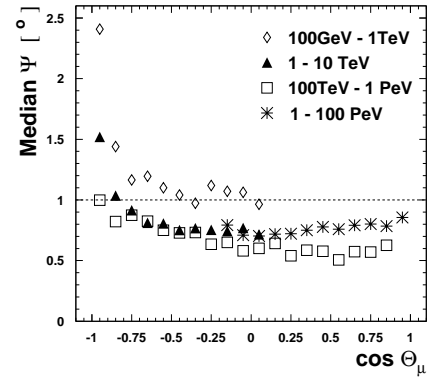


Figure 5: Pointing resolution (median space angle) for neutrino-induced muon events as a function of zenith angle

Fig. 6 shows the energy spectra of selected neutrinos for E^{-2} sources. (Note that Fig. 4 refers to muon energy, but Fig. 6 to neutrino energy). The top part shows the spectrum after fake event rejection and after cuts tailored to get best sensitivity to *point sources*. It confirms the TeV threshold demonstrated in Fig. 4. The bottom part shows the spectrum if the cuts are optimized for best sensitivity to a *diffuse* E^{-2} flux. Clearly the

large background from atmospheric neutrinos over 2π or more requires harder energy cuts than in the case of point sources. The threshold is now about 100 times higher than for the point source analysis.

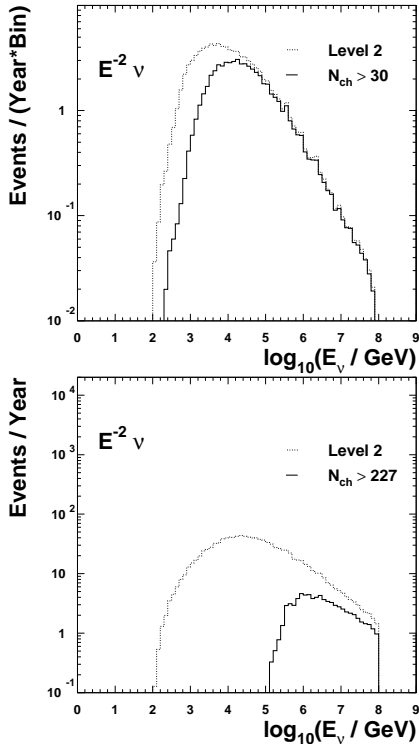


Figure 6: Energy spectra of selected neutrinos for a E^{-2} source. Cuts have been optimized to get the best sensitivity to point sources (top) and to a diffuse flux (bottom). The cutoff at 10^8 GeV is due to the limited energy range of the simulation.

Fig. 7 shows the expected sensitivity to diffuse fluxes as function of neutrino energy. Solid lines indicate the expected 90% c.l. limits for E^{-2} and E^{-1} spectra, respectively, calculated for a data taking period of three years. The lines extend over the energy range containing 90% of the expected signal. The dashed lines indicate the Stecker and Salamon model for photo-hadronic interactions in AGN cores [13]. The dotted line corresponds to the Mannheim, Protheroe and Rachen model on neutrino emission from photo-hadronic interactions in AGN jets [14]. In case of no signal, these models could be rejected with model rejection factor (mrf) [15] of 10^{-3} and 10^{-2} respectively. Also shown is the GRB estimate by Waxman and Bahcall [16] which would yield of the order of ten events coinciding with a GRB, for 1000 GRBs monitored.

Apart from tracks, IceCube can map *cascades*, with an energy resolution of about 30% at high energies. Compared to Amanda, IceCube has a much larger central volume shielded by outer “veto layers”. This allows significantly better recognition of isolated cascades – an important issue for the detection of ν_e or ν_τ interactions.

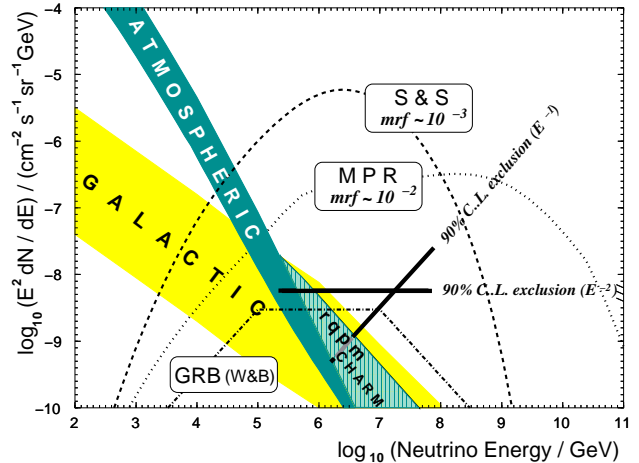


Figure 7: Expected sensitivities of the IceCube detector. See text for explanations.

VI. POSSIBLE EXTENSIONS

Parallel to the implementation of the IceCube baseline design, methods are studied to extend the capabilities of the South Pole detector towards higher as well as towards lower energies. With a volume of a cubic kilometer, IceCube will surpass Amanda by a factor of 40 (and Super-K by a factor of 1000). These numbers refer to the sensitivity in the energy range of TeV-PeV.

For energies below a few hundred GeV the light emission is too low to fire many PMTs, and the effective volume decreases drastically. In order to increase the sensitivity at lower energies, more light has to be collected. First encouraging result have been obtained in production of transparent hats for the glass spheres housing the PMTs. These hats are doped with wavelength shifter which moves the light from wavelengths below 300 nm to wavelengths above 320 nm where the spheres are becoming transparent [7]. The resulting increase in light collection may be as high as 40%, following first measurements and estimates. This would result in a lower energy threshold and better reconstruction.

For energies above 100 PeV, on the other hand, expected neutrino fluxes are so small that even a cubic kilometer is not sufficient to catch a few events. Instead, volumes of ten or hundred cubic kilometers are required. With the given spacing of PMTs (17 m vertically, 125 m horizontally) this is not affordable, neither logistically nor financially. A larger volume could be reached by larger PMT spacing (see e.g. [8]). The increase of distance, however, is limited by the absorption length of light (~ 100 m) and the smaller amount of light reaching the PMTs. In order to allow a much larger spacing, an information carrier with smaller absorption in ice than light has to be used. Radio wave detection has been successfully applied to derive ultra-high energy flux limits with the RICE experiment, located above the Amanda experiment, at a depth of a few hundred meters [17]. Another method is the detection of acoustic

waves generated in high-energy particle cascades. The attenuation length of this signal in pure ice at -40°C is about 2 km [18]. R&D work is underway to develop sensitive acoustic sensors with good signal-to-noise behaviour, to test them at accelerators, and to understand noise behaviour in open reservoirs of water and ice [19]. In-ice tests will show how well the method will work in natural ice.

VII. STATUS AND OUTLOOK

The IceCube collaboration includes about 150 scientists from institutions in Belgium, Germany, Japan, Netherlands, New Zealand, Sweden, UK, USA and Venezuela. In the USA IceCube is handled as MRE (Major Research Equipment) project of the National Science Foundation, NSF. Funding of the start-up phase started in FY 2002. In the mean time, the project moved from the start-up phase to the implementation phase and is now fully installed as a MRE project. Apart from the US budget, significant funding has been approved in Belgium, Germany and Sweden.

The present plan foresees transportation of the EHWD to the Pole at the end of 2004, and drilling of a few first holes in January 2005. Amanda will be integrated into the year-by-year increasing IceCube. The growing detector will take data during construction, with each string coming online within days after deployment. Construction of IceCube is to be completed in 2010, followed by ~ 10 years of data taking.

IceCube Author List

A. Achterberg²⁵, M. Ackermann⁶, J. Ahrens¹⁵, J.N. Bahcall⁸, X. Bai¹, R.C. Bay¹⁴, T. Becka¹⁵, K.-H. Becker², J. Bergmans²⁵, D. Berley¹⁶, E. Bernardini⁶, D. Bertrand³, D.Z. Besson⁹, E. Blaufuss¹⁶, D.J. Boersma⁶, S. Böser⁶, C. Bohm²⁶, O. Botner²⁴, A. Bouchta²⁴, O. Bouhali³, T. Burgess²⁶, W. Carithers¹⁰, T. Castermans¹⁸, J. Cavin²², W. Chinowsky¹⁰, D. Chirkin¹⁴, B. Collin¹², J. Conrad²⁴, J. Cooley²¹, D.F. Cowen¹², A. Davour²⁴, C. De Clercq²⁷, T. DeYoung¹⁶, P. Desiati²¹, R. Ehrlich¹⁶, R.W. Ellsworth¹⁷, P.A. Evenson¹, A.R. Fazely¹³, T. Feser¹⁵, T.K. Gaissler¹, J. Gallagher²⁰, R. Ganugapati²¹, H. Geenen², A. Goldschmidt¹⁰, J.A. Goodman¹⁶, R.M. Gunasingha¹³, A. Hallgren²⁴, F. Halzen²¹, K. Hanson²¹, R. Hardtke²¹, T. Hauschildt⁶, D. Hays¹⁰, K. Helbing¹⁰, M. Hellwig¹⁵, P. Herquet¹⁸, G.C. Hill²¹, D. Hubert²⁷, B. Hughey²¹, P.O. Hulth²⁶, K. Hultqvist²⁶, S. Hundertmark²⁶, J. Jacobsen¹⁰, G.S. Japaridze⁴, A. Jones¹⁰, A. Karle²¹, H. Kawai⁵, M. Kestel¹², N. Kitamura²², R. Koch²², L. Köpke¹⁵, M. Kowalski⁶, J.I. Lamoureux¹⁰, N. Langer²⁵, H. Leich⁶, I. Liubarsky⁷, J. Madsen²³, K. Mandli²¹, H.S. Matis¹⁰, C.P. McParland¹⁰, T. Messarius², P. Mészáros^{11,12}, Y. Minaeva²⁶, R.H. Minor¹⁰, P. Miočinić¹⁴, H. Miyamoto⁵, R. Morse²¹, R. Nahnauer⁶, T. Neunhoffer¹⁵, P. Niessen²⁷, D.R. Nygren¹⁰, H. Ögelman²¹, Ph. Olbrechts²⁷, S. Patton¹⁰, R. Paulos²¹, C. Pérez de los Heros²⁴, A.C. Pohl²⁶, J. Pretz¹⁶, P.B. Price¹⁴, G.T. Przybylski¹⁰, K. Rawlins²¹, S. Razzaque¹¹, E. Resconi⁶, W. Rhode², M. Ribordy¹⁸, S. Richter²¹, H.-G. Sander¹⁵, K. Schinarakis², S. Schlenstedt⁶, D. Schneider²¹, R. Schwarz²¹, D. Seckel¹, A.J. Smith¹⁶, M. Solarz¹⁴, G.M. Spiczak²³, C. Spiering⁶, M. Stamatikos²¹, T. Stanev¹, D. Steele²¹, P. Steffen⁶, T. Stetzelberger¹⁰, R.G. Stokstad¹⁰, K.-H. Sulanke⁶, G.W. Sullivan¹⁶, T.J. Sumner⁷, I. Taboada¹⁹, S. Tilav¹, N. van Eijndhoven²⁵, W. Wagner², C. Walck²⁶, Y.-R. Wang²¹, C.H. Wiebusch², C. Wiedemann²⁶, R. Wischniewski⁶, H. Wissing⁶, K. Woschnagg¹⁴, S. Yoshida⁵

(1) Bartol Research Institute, University of Delaware, Newark, DE 19716,

USA

- (2) Fachbereich 8 Physik, BUGH Wuppertal, D-42097 Wuppertal, Germany
- (3) Université Libre de Bruxelles, Science Faculty CP230, Boulevard du Triomphe, B-1050 Brussels, Belgium
- (4) CTSPS, Clark-Atlanta University, Atlanta, GA 30314, USA
- (5) Dept. of Physics, Chiba University, Chiba 263-8522 Japan
- (6) DESY-Zeuthen, D-15738 Zeuthen, Germany
- (7) Blackett Laboratory, Imperial College, London SW7 2BW, UK
- (8) Institute for Advanced Study, Princeton, NJ 08540, USA
- (9) Dept. of Physics and Astronomy, University of Kansas, Lawrence, KS 66045, USA
- (10) Lawrence Berkeley National Laboratory, Berkeley, CA 94720, USA
- (11) Dept. of Astronomy and Astrophysics, Pennsylvania State University, University Park, PA 16802, USA
- (12) Dept. of Physics, Pennsylvania State University, University Park, PA 16802, USA
- (13) Dept. of Physics, Southern University, Baton Rouge, LA 70813, USA
- (14) Dept. of Physics, University of California, Berkeley, CA 94720, USA
- (15) Institute of Physics, University of Mainz, Staudinger Weg 7, D-55099 Mainz, Germany
- (16) Dept. of Physics, University of Maryland, College Park, MD 20742, USA
- (17) Dept. of Physics, George Mason University, Fairfax, VA 22030, USA
- (18) University of Mons-Hainaut, 7000 Mons, Belgium
- (19) Departamento de Física, Universidad Simón Bolívar, Caracas, 1080, Venezuela
- (20) Dept. of Astronomy, University of Wisconsin, Madison, WI 53706, USA
- (21) Dept. of Physics, University of Wisconsin, Madison, WI 53706, USA
- (22) SSEC, University of Wisconsin, Madison, WI 53706, USA
- (23) Physics Dept., University of Wisconsin, River Falls, WI 54022, USA
- (24) Division of High Energy Physics, Uppsala University, S-75121 Uppsala, Sweden
- (25) Faculty of Physics and Astronomy, Utrecht University, NL-3584 CC Utrecht, The Netherlands
- (26) Dept. of Physics, Stockholm University, SE-10691 Stockholm, Sweden
- (27) Vrije Universiteit Brussel, Dienst ELEM, B-1050 Brussels, Belgium

REFERENCES

- [1] <http://icecube.wisc.edu>
- [2] J.Ahrens et al., accepted by Astroparticle Physics, astro-ph/0305196
- [3] C.Spiering for the Amanda collaboration, Proc. 27th ICRC (2001) 1242.
- [4] F.Halzen, astro-ph/0311004.
- [5] see E.Bernardini, talk at this workshop.
- [6] M.Leuthold, Proc. Workshop on Large Neutrino Telescopes, Zeuthen 1998, <http://www.ifh.de/nuastro/publications/conferences/proc.html>
- [7] E. Resconi, paper to be presented at the Xth Vienna Conference on Instrumentation.
- [8] F.Halzen and D.Hooper, astro-ph/0310152
- [9] R.G.Stokstad et al., Preprint LBNL-43200, Berkeley 1998.
- [10] C.Spiering, Journ.Phys.G: Nucl.Part.Phys.29 (2003), astro-ph/030368.
- [11] S.Yoshida, R.Ishibashi, H.Miyamoto, astro-ph/0312078, to be subm. to Phys.Rev.D.
- [12] see also C.Wiebusch, talk at this workshop.
- [13] F.W.Stecker and M.H.Salamon, Space Sci.Rev.75 (1996) 341.
- [14] K.Mannheim, R.Protheroe, J.Rachen, Phys.Rev.D63 (2001) 023003.
- [15] G.G.Hill and K.Rawlins, Astropart.Phys.19 (2003) 393.
- [16] E.Waxmann, J.Bahcall, Phys.Rev.D59 (1999)023002.
- [17] I.Kravtchenko et al., Astroparticle Physics 20 (2003) 195 and astro-ph/0206371
- [18] P.B.Price, Astropart.Phys.5 (1996) 43.
- [19] R.Nahnauer, <http://hep.stanford.edu/neutrino/SAUND/workshop/slides/>